

Cyclopentadienyl Chromium β -Diketiminate Complexes: Initiators, Ligand Steric Effects, and Deactivation Processes in the Controlled Radical Polymerization of Vinyl Acetate

Yohan Champouret,[†] K. Cory MacLeod,[‡] Ulrich Baisch,[†] Brian O. Patrick,[§]
Kevin M. Smith,^{*,‡} and Rinaldo Poli^{*,†,⊥}

[†]CNRS, LCC (Laboratoire de Chimie de Coordination), Université de Toulouse, UPS, INPT, 205 Route de Narbonne, F-31077 Toulouse, France, [‡]Department of Chemistry, University of British Columbia Okanagan, 3333 University Way, Kelowna, British Columbia, Canada V1V 1V7, [§]Department of Chemistry, University of British Columbia, Vancouver, British Columbia, Canada V6T 1Z1, and [⊥]Institut Universitaire de France, 103 Boulevard Saint-Michel, 75005 Paris, France

Received October 7, 2009

The new compounds CpCr(nacnac^{Ar,Ar'}) with nacnac^{Ar,Ar'} = Ar–N=C(Me)–CHC(Me)–N–Ar' (Ar = Ar' = C₆H₂Me₃-2,4,6 or mes, **2**; C₆H₃Et₂-2,6 or dep, **3**; Ar = C₆H₃Me₂-2,6 or xyl and Ar' = C₆H₃iPr-2,6 or dipp, **4**) have been synthesized and used in polymerization experiments in addition to the previously known analogues with Ar = Ar' = xyl, **1**, or dipp, **5**. The compounds were used as moderators for the polymerization of vinyl acetate (VAc) initiated by V-70, according to an OMRP mechanism. The alkylchromium(III) thermal initiator CpCr(nacnac^{xyl,xyl})(CH₂CMe₃) (**8**) was synthesized from CpCr(nacnac^{xyl,xyl})(OTs) (**7**) and Mg(CH₂CMe₃)₂(dioxane), while **7** was obtained from CpCr(nacnac^{xyl,xyl})Cl (**6**) and AgOTs. The polymerizations carried out with (**1–5**)/V-70/VAc at elevated temperatures yielded rapid deactivation, suggestive of irreversible radical trapping. On the other hand, room-temperature polymerizations carried out with **6**/VAc proceeded, albeit slowly, to greater conversions. A labilizing effect of the Ar/Ar' steric bulk is suggested by QM/MM calculations of Cr^{III}–C BDE for models of the OMRP dormant species with **1**, **5**, and the parent system where Ar = Ar' = Ph. Thermal deactivation of the nacnac^{xyl,xyl} system has been evidenced, with formation of the acetate complex CpCr(nacnac^{xyl,xyl})(OAc), **9**, as confirmed by an UV–vis study and by independent synthesis. This product is proposed to form by β -acetate transfer from the growing radical chain, triggered by a head–head monomer insertion. Compounds **2**, **3**, **6**, **7**, **8**, and **9** have been structurally characterized by X-ray diffraction methods.

Introduction

The controlled polymerization of functionalized monomers such as vinyl acetate continues to pose a formidable challenge to transition metal chemists. Early metal catalysts that effectively polymerize nonpolar monomers by an insertion mechanism are incompatible with vinyl ester substrates.¹ More functional group tolerant late metal catalysts experience problems in copolymerization of vinyl acetate and ethylene due to low π -bonding affinity, chelate formation, and β -acetate elimination.^{2–4} Vinyl acetate is also a difficult monomer for controlled radical polymerization methods due to the relatively high reactivity of the propagating radical species compared to more tractable substrates such as styrene or methyl acrylate.⁵

Organometallic radical polymerization (OMRP) provides a new route to poly(vinylacetate). In the OMRP mechanism, unwanted bimolecular radical coupling reactions are effectively prevented by reversible formation and homolytic cleavage of metal–alkyl bonds.⁶ Cobalt-mediated radical polymerization is the most well explored system for OMRP of vinyl acetate. The mechanistic details of these polymerizations are rather complex, with a range of termination and chain transfer steps playing a role dictated by the degree of solvent coordination and the spin state of the Co(II) and Co(III) intermediate species.⁷

In principle, well-defined high-spin Cr^{II} and Cr^{III} complexes could serve as a simpler system for preparing poly(vinylacetate) via OMRP. Chromium(II) species such as aqueous [Cr(H₂O)₆]²⁺ or CrCl₂ in coordinating aprotic solvents have long been known to effectively trap organic radicals at close to diffusion-controlled rates to form Cr^{III}-alkyl intermediates.⁸ This fundamental reactivity mode is the key step in the chromium-mediated coupling of organic

*Corresponding authors. E-mail: kevin.m.smith@ubs.ca.

(1) Chen, E. Y.-X. *Chem. Rev.* **2009**, *109*, 5157–5214.
(2) Williams, B. S.; Leatherman, M. D.; White, P. S.; Brookhart, M. *J. Am. Chem. Soc.* **2005**, *127*, 5132–5146.
(3) Berkefeld, A.; Drexler, M.; Möller, H. M.; Mecking, S. *J. Am. Chem. Soc.* **2009**, *131*, 12613–12622.
(4) (a) Ito, S.; Munakata, K.; Nakamura, A.; Nozaki, K. *J. Am. Chem. Soc.* **2009**, *131*, 14606–14607. (b) Nakamura, A.; Ito, S.; Nozaki, K. *Chem. Rev.* **2009**, *109*, 5215–5244.
(5) Satoh, K.; Kamigaito, M. *Chem. Rev.* **2009**, *109*, 5120–5156.

(6) Poli, R. *Angew. Chem., Int. Ed.* **2006**, *45*, 5058–5070.
(7) Debuigne, A.; Poli, R.; Jérôme, C.; Jérôme, R.; Detrembleur, C. *Prog. Polym. Sci.* **2009**, *34*, 211–239.
(8) Smith, K. M. *Coord. Chem. Rev.* **2006**, *250*, 1023–1031.

halides and aldehydes.^{9,10} The homolytic bond dissociation energy (BDE) of a Cr^{III}–alkyl bond is typically greater than that of a Co^{III}–alkyl. Homolytic transfer of alkyl groups from Co^{III}–R to Cr^{II} is used in the Takai–Utimoto reaction, where catalytic amounts of B₁₂ or cobalt phthalocyanine are used to activate alkyl halides and transfer the organic radical from Co to Cr prior to coupling with aldehydes.¹¹ While the trapping of organic radicals with Cr^{II} to form octahedral Cr^{III} organometallic species is usually considered to be rapid and irreversible, the reaction can be reversible for secondary or tertiary radicals due to the lowering of the Cr–R BDE through adverse steric interactions.^{12,13}

CpCr(nacnac) complexes are high-spin, well-characterized species that do not bind coordinating solvents but have been shown to trap CH₃ radicals.^{14,15} CpCr(nacnac)(CH₃) complexes can be independently synthesized by the reaction of Grignard reagents with the corresponding Cr^{III} triflate or halide compounds. Modifying the size of the *ortho* substituents of the nacnac N-aryl groups should exert a dramatic influence on the Cr^{III}–R BDE for CpCr(nacnac)R complexes, as indicated by preliminary DFT calculations.¹⁶ This desired tunability of the M–R BDE is critical for both exploring structure–activity relationships for these reagents and developing a class of well-defined organometallic complexes capable of mediating OMRP reactions for a range of activated olefin substrates.⁶

In 2008, we communicated our preliminary studies toward OMRP of vinyl acetate using CpCr(nacnac) complexes and V-70.¹⁶ In this paper, we further examine the structure–activity relationships of vinyl acetate polymerization using isolated CpCr(nacnac) compounds with V-70. Although the paramagnetic nature of the Cr^{II} and Cr^{III} complexes makes interpretation of their NMR spectra difficult, the UV–vis spectra of these intensely colored species proved to be quite informative. Employing elevated temperatures to accelerate initiation in the CpCr(nacnac)/V-70/vinyl acetate system unexpectedly led to a decrease in the observed rate of polymerization due to formation of an inactive Cr^{III} acetate thermal decomposition product. As an alternative to thermolysis of CpCr(nacnac) with V-70, a well-defined Cr^{III} neopentyl complex was developed as a single-component OMRP reagent. The choice of the neopentyl group was based on the high steric demand of this specific alkyl ligand,

which has long been used to provoke unique organometallic reactivity, both of nonradical^{17–20} and of radical type.^{21–23}

Experimental Section

Materials. All reactions, unless otherwise stated, were carried out under dry, oxygen-free argon or nitrogen, using standard Schlenk and glovebox techniques. Solvents were dried by using the method of Grubbs,²⁴ or they were distilled under argon from appropriate drying agents and degassed by three freeze–vacuum–thaw cycles prior to use.²⁵ Celite (Aldrich) was dried overnight at 110 °C before being evacuated and then stored under argon or nitrogen. Vinyl acetate (VAc, 99%, Alfa Aesar or 99+%, Aldrich) was passed through a neutral alumina column to remove the stabilizer, dried over calcium hydride, distilled at 90 °C, degassed by three freeze–vacuum–thaw cycles, and stored under argon or nitrogen at –20 °C. 2,2'-Azobis(4-methoxy-2,4-dimethylvaleronitrile) (V-70, 96%, Wako) was used as received. *n*BuLi (1.6 M in hexanes), *p*-toluenesulfonic acid monohydrate, acetylacetonate, 2,6-dimethylaniline, 2,6-diisopropylaniline, 2,6-diethylaniline, 2,4,6-trimethylaniline, CrCl₃ (anhydrous), 1,4-dioxane, silver *p*-toluenesulfonate, and silver acetate were purchased from Aldrich and used as received. The symmetric β -diketiminato ligands (2,6-Me₂C₆H₃)NHC(Me)CHC(Me)N(2,6-Me₂C₆H₃),²⁶ (2,6-Et₂C₆H₃)NHC(Me)CHC(Me)N(2,6-Et₂C₆H₃),²⁷ and (2,4,6-Me₃C₆H₂)NHC(Me)CHC(Me)N(2,4,6-Me₃C₆H₂)²⁷ and the mixed N-aryl β -diketiminato ligand (2,6-*i*Pr₂C₆H₃)NHC(Me)CHC(Me)N(2,6-Me₂C₆H₃)²⁸ were prepared according to the literature procedures. NaCp was prepared according to the literature procedure²⁹ or was purchased from Aldrich as a 2.0 M solution in THF and used as received. Compounds Mg(CH₂CMe₃)₂·*x*(1,4-dioxane),³⁰ CrCl₂(tmeda),³¹ **1**,¹⁶ and **5**¹⁶ were prepared according to literature procedures.

Characterizations. ¹H NMR spectra were recorded on a Bruker ARX 250 or a Bruker DPX 300 spectrometer. A Varian Cary 100 Bio UV–visible spectrophotometer was used to conduct measurements using a specially constructed cell for air-sensitive samples: a Kontes Hi-Vac Valve with PTFE plug was attached by a professional glassblower to a Hellma 10 mm path length quartz absorption cell with a quartz-to-glass graded seal. Size exclusion chromatography (SEC) of poly(vinyl acetate) was carried out in filtered THF (flow rate: 1 mL/min) at 35 °C on a 300 × 7.5 mm PL gel 5 μ m mixed-D column (Polymer Laboratories), equipped with multiangle light scattering (miniDawn Tristar, Wyatt Technology Corporation) and refractive index (RI2000, Sopares) detectors, with a Waters column pack (300 × 7.5 mm, Ultrastaygel 104, 103, 100 Å), equipped with multiangle light scattering (miniDawn Tristar, Wyatt Technology Corp.) and refractive index (waters 410) detectors or at 30 °C on a Polymer Laboratories PL-GPC 50 Plus (two PLgel mixed-C columns in series) with a PL-AS RT autosampler and PL-RI detector. The isolated polymer samples were dissolved in THF, and the polymer solutions were filtered

(9) Furstner, A. *Chem. Rev.* **1999**, *99*, 991–1046.

(10) Wessjohann, L. A.; Scheid, G. *Synthesis* **1999**, 1–36.

(11) Takai, K.; Nitta, K.; Fujimura, O.; Utimoto, K. *J. Org. Chem.* **1989**, *54*, 4732–4734.

(12) Takai, K.; Matsukawa, N.; Takahashi, A.; Fujii, T. *Angew. Chem., Int. Ed.* **1998**, *37*, 152–155.

(13) Wessjohann, L. A.; Schmidt, G.; Schrekker, H. S. *Tetrahedron* **2008**, *64*, 2134–2142.

(14) Doherty, J. C.; Ballem, K. H. D.; Patrick, B. O.; Smith, K. M. *Organometallics* **2004**, *23*, 1487–1489.

(15) MacLeod, K. C.; Conway, J. L.; Tang, L.; Smith, J. J.; Corcoran, L. D.; Ballem, K. H. D.; Patrick, B. O.; Smith, K. M. *Organometallics* **2009**, *28*, 6798–6806.

(16) Champouret, Y.; Baisch, U.; Poli, R.; Tang, L.; Conway, J. L.; Smith, K. M. *Angew. Chem., Int. Ed.* **2008**, *47*, 6069–6072.

(17) Schrock, R. R. *Acc. Chem. Res.* **1979**, *12*, 98–104.

(18) Foley, P.; DiCosimo, R.; Whitesides, G. M. *J. Am. Chem. Soc.* **1980**, *102*, 6713–6725.

(19) Pamplin, C. B.; Legzdins, P. *Acc. Chem. Res.* **2003**, *36*, 223–233.

(20) Mindiola, D. J. *Acc. Chem. Res.* **2006**, *39*, 813–821.

(21) Tsou, T.-T.; Loots, M.; Halpern, J. J. *J. Am. Chem. Soc.* **1982**, *104*, 623–624.

(22) Wayland, B. B.; Poszmik, G.; Mukerjee, S.; Fryd, M. *J. Am. Chem. Soc.* **1994**, *116*, 7943–7944.

(23) Fernandez, I.; Trovitch, R. J.; Lobkovsky, E.; Chirik, P. J. *Organometallics* **2008**, *27*, 109–118.

(24) Pangborn, A. B.; Giardello, M. A.; Grubbs, R. H.; Rosen, R. K.; Timmers, F. J. *Organometallics* **1996**, *15*, 1518–1520.

(25) Armarego, W. L. F.; Perrin, D. D. *Purification of Laboratory Chemicals*, 4th ed.; Butterworth Heinemann, 1996.

(26) Budzelaar, P. H. M.; de Gelder, R.; Gal, A. W. *Organometallics* **1998**, *17*, 4121–4123.

(27) Cheng, M.; Moore, D. R.; Reczek, J. J.; Chamberlain, B. M.; Lobkovsky, E. B.; Coates, G. W. *J. Am. Chem. Soc.* **2001**, *123*, 8738–8749.

(28) Gong, S. G.; Ma, H. Y. *Dalton Trans.* **2008**, 3345–3357.

(29) Panda, T. K.; Gamer, M. T.; Roesky, P. W. *Organometallics* **2003**, *22*, 877–878.

(30) (a) Andersen, R. A.; Wilkinson, G. J. *Chem. Soc., Dalton Trans.* **1977**, 809–811. (b) Dryden, N. H.; Legzdins, P.; Trotter, J.; Yee, V. C. *Organometallics* **1991**, *10*, 2857–2870.

(31) Hao, S. K.; Song, J. I.; Berno, P.; Gambarotta, S. *Organometallics* **1994**, *13*, 1326–1335.

(pore size = 0.45 μm) before chromatographic analysis. The columns were calibrated against linear polystyrene standards (Polymer Laboratories). Elemental analyses were performed by Guelph Chemical Laboratories, Guelph, ON, Canada. Solution magnetic susceptibilities were determined by the Evans method.³²

Synthesis of CpCr(nacnac^{mes,mes}) (2). Following a procedure similar to that previously reported for compound **1**,¹⁶ compound (2,4,6-Me₃C₆H₂)NHC(Me)CHC(Me)N(2,4,6-Me₃C₆H₂) (744 mg, 2.23 mmol) was dissolved in THF (12 mL). *n*-BuLi (1.60 mL, 2.56 mmol, 1.15 equiv) was added dropwise, and the resulting yellow solution was stirred for 30 min at room temperature. In a separate Schlenk flask, CrCl₂(tmeda) (531 mg, 2.22 mmol, 1 equiv) was suspended in THF (35 mL) followed by the addition of NaCp (1.25 mL, 2.50 mmol, 1.13 equiv). The resulting mixture was stirred for 30 min at room temperature. To this solution was added dropwise the lithium salt prepared above, and the mixture was stirred at room temperature overnight. The solvent was evaporated *in vacuo*, and the residue was extracted with hexanes, followed by filtration through Celite. The solvent was again removed *in vacuo*, and the complex was dissolved in hexanes (20 mL), filtered, and cooled to -35 °C for several days. Black crystals (730 mg) were isolated in two crops. Yield: 73%. μ_{eff} (Evans, C₆D₆): 4.8(1) μ_{B} . Anal. Calcd for C₂₈H₃₄CrN₂: C, 74.64; H, 7.61; N, 6.22. Found: C, 74.83; H, 7.96; N, 6.42. UV/vis (hexanes; λ_{max} , nm (ϵ , M⁻¹ cm⁻¹)): 308 (11 700), 427 (7210), 573 (376).

Synthesis of CpCr(nacnac^{dep,dep}) (3). Following a procedure similar to that previously reported for compound **1**,¹⁶ compound (2,6-Et₂C₆H₃)NHC(Me)CHC(Me)N(2,6-Et₂C₆H₃) (1.00 g, 2.76 mmol) was dissolved in THF (10 mL) and cooled to -40 °C in an acetonitrile/liquid nitrogen bath. *n*-BuLi (1.75 mL, 2.80 mmol, 1.01 equiv) was added dropwise, and the resulting yellow solution was stirred for one hour at -40 °C. In a separate Schlenk flask, CrCl₂(tmeda) (660 mg, 2.76 mmol, 1 equiv) and NaCp (243 mg, 2.76 mmol, 1 equiv) were suspended in THF (15 mL) and the contents stirred for 20 min at room temperature. To this solution was added dropwise via a cannula the lithium salt prepared above, and the mixture was stirred at room temperature overnight. The solvent was evaporated *in vacuo*, and the residue was extracted with pentane, followed by filtration through Celite. The solvent was again removed *in vacuo*, and the complex was dissolved in the minimum amount of pentane, filtered, and cooled to -80 °C overnight to yield 462 mg of black crystals. Yield: 35%. μ_{eff} (Evans, C₆D₆): 4.6(1) μ_{B} . Anal. Calcd for C₃₀H₃₈CrN₂: C, 75.28; H, 8.00; N, 5.85. Found: C, 74.97; H, 8.30; N, 5.96. UV/vis (hexanes; λ_{max} , nm (ϵ , M⁻¹ cm⁻¹)): 308 (12 200), 428 (7910), 576 (411).

Synthesis of CpCr(nacnac^{xy1,dipp}) (4). Using a procedure identical to that described above for compound **2**, compound CpCr(nacnac^{xy1,dipp}) (**4**, 223 mg) was obtained as black crystals from (2,6-*i*Pr₂C₆H₃)NHC(Me)CHC(Me)N(2,6-Me₂C₆H₃) (316 mg, 0.872 mmol). Yield: 54%. μ_{eff} (Evans, C₆D₆): 4.4(1) μ_{B} . Anal. Calcd for C₃₀H₃₈CrN₂: C, 75.28; H, 8.00; N, 5.85. Found: C, 75.00; H, 8.38; N, 5.62.

Synthesis of CpCr(nacnac^{xy1,xy1})Cl (6). Compound (2,6-Me₂C₆H₃)NHC(Me)CHC(Me)N(2,6-Me₂C₆H₃) (1.43 g, 4.67 mmol) was added to a Schlenk flask, dissolved in THF (30 mL), and cooled to 0 °C in an ice-water bath. *n*-BuLi (3.20 mL, 5.12 mmol, 1.10 equiv) was added dropwise, and the resulting yellow solution was allowed to warm to room temperature while stirring for 1 h. The lithium salt was then cannulated into a suspension of CrCl₃ (744 mg, 4.70 mmol, 1.00 equiv) in THF (20 mL) and stirred at room temperature overnight. NaCp (2.60 mL, 5.20 mmol, 1.11 equiv) was added to the solution, which was again stirred at room temperature overnight. The solvent was evaporated *in vacuo*, and the residue was extracted with 40 mL of a hexanes/dichloromethane mixture (3:1), filtered through Celite, and rinsed with hexanes (3 \times 5 mL).

The green to incident and orange to transmitted light filtrate was concentrated and cooled to -20 °C to yield 1.66 g of dark green crystals over several days in three crops. Yield: 78%. Anal. Calcd for C₂₆H₃₀CrN₂Cl: C, 68.19; H, 6.60; N, 6.12. Found: C, 67.88; H, 6.50; N, 5.73. UV/vis (hexanes; λ_{max} , nm (ϵ , M⁻¹ cm⁻¹)): 418 (7220), 581 (504).

Synthesis of CpCr(nacnac^{xy1,xy1})OTs (7). Compound **6** (1.28 g, 2.79 mmol) and AgOTs (781 mg, 2.80 mmol, 1.00 equiv) were placed in a Schlenk flask followed by the addition of THF (60 mL). The mixture was stirred overnight at room temperature and filtered through Celite, and the solvent was evaporated *in vacuo*. The residue was extracted with 32 mL of a hexanes/dichloromethane mixture (4:1), filtered through Celite, and rinsed with hexanes (2 \times 5 mL). The green to incident and orange to transmitted light filtrate was cooled to -20 °C to yield 1.40 g of black crystals over several days in four crops. Yield: 84%. Anal. Calcd for C₃₃H₃₇CrO₃N₂S: C, 66.76; H, 6.28; N, 4.72. Found: C, 66.50; H, 6.20; N, 4.34. UV/vis (diethyl ether; λ_{max} , nm (ϵ , M⁻¹ cm⁻¹)): 411 (8140), 571 (548).

Synthesis of CpCr(nacnac^{xy1,xy1})CH₂CMe₃ (8). Compound **7** (600 mg, 1.01 mmol) was added to a Schlenk flask followed by the addition of diethyl ether (30 mL). Mg(CH₂CMe₃)₂ · 1.05(1,4-dioxane) (143 mg, 0.554 mmol, 0.549 equiv) in diethyl ether (5 mL) was added dropwise to the Schlenk. The mixture was stirred for 1.5 h at room temperature, the solvent was evacuated *in vacuo*, and the residue was extracted with hexanes (30 mL), filtered through Celite, and rinsed with hexanes (3 \times 5 mL). The solvent was again evacuated *in vacuo*, and the residue was extracted with hexanes (15 mL), filtered, and cooled to -35 °C to yield 335 mg of black crystals over several days in four crops. Yield: 67%. Anal. Calcd for C₃₁H₄₁CrN₂: C, 75.42; H, 8.37; N, 5.67. Found: C, 75.27; H, 8.69; N, 5.66. UV/vis (hexanes; λ_{max} , nm (ϵ , M⁻¹ cm⁻¹)): 404 (5170), 567 (1050).

Synthesis of CpCr(nacnac^{xy1,xy1})OC(O)Me (9). Compound **6** (259 mg, 0.566 mmol) and AgOAc (95.2 mg, 0.570 mmol, 1.01 equiv) were placed in a Schlenk flask followed by the addition of THF (20 mL). The mixture was stirred overnight at room temperature in the absence of light, the solvent was evacuated *in vacuo*, and the residue was extracted with 12 mL of a hexanes/dichloromethane mixture (3:1), filtered through Celite, and rinsed with hexanes (3 \times 3 mL). The green filtrate was concentrated slightly and cooled to -20 °C to yield 187 mg of black crystals over several days in three crops. Yield: 69%. UV/vis (hexanes; λ_{max} , nm (ϵ , M⁻¹ cm⁻¹)): 411 (9160), 508 (446), 588 (574).

General Procedures for the Radical Polymerization of Vinyl Acetate. **a. OMRP Procedure: Cr^{II} + V-70.** All polymerizations were conducted following the same experimental protocol. A typical experiment is described here as a representative example with complex **4** (Cr:V-70:VAc = 1:0.8:500). All operations were carried out under a protective argon atmosphere. Complex **4** (41 mg, 0.086 mmol, 1 equiv) and V-70 (18.7 mg 0.061 mmol, 0.8 equiv) were introduced in a Schlenk tube, followed by the addition of degassed vinyl acetate (4 mL, 43 mmol, 500 equiv). The Schlenk tube was degassed by three freeze-vacuum-thaw cycles and then immersed in an oil bath preheated at 50 °C. At the desired time, the Schlenk flask was rapidly cooled to room temperature by immersion into iced water before sample withdrawal. The monomer conversion was determined gravimetrically after removal of the unconverted monomer under reduced pressure, and the resulting residue was used for SEC characterization.

b. OMRP Procedure: Cr^{III}-Np. The experimental protocol is similar to that described above for the OMRP Procedure: Cr^{II} + V-70. As an example, complex **8** (17.5 mg, 0.035 mmol, 1 equiv) and VAc (4 mL, 43 mmol, 1200 equiv) were introduced into a Schlenk flask and stirred at room temperature. At the desired time, a sample was removed from the Schlenk flask and analyzed as described above.

X-ray Crystallography. A single crystal of each compound was mounted on a glass fiber and centered on the optical path of

(32) (a) Baker, M. V.; Field, L. D.; Hambly, T. W. *Inorg. Chem.* **1988**, *27*, 2872–2876. (b) Schubert, E. M. *J. Chem. Educ.* **1992**, *69*, 62.

a Bruker X8 APEX II diffractometer with graphite-monochromated Mo K α radiation. The data were collected at a temperature of -100.0 ± 0.1 °C in a series of ϕ and ω scans in 0.50° oscillations. Data were collected and integrated using the Bruker SAINT software package³³ and were corrected for absorption effects using the multiscan technique (SADABS)³⁴ and for Lorentz and polarization effects. All structures were solved by direct methods with SIR97.³⁵ For structures **2**, **3**, and **6** the Cp ring was found disordered among different orientations (four for **2** and two for **3** and **6**). Two of the four orientations in **2** are symmetry-related to the other two since the molecule sits on a 2-fold axis with a half-molecule in the asymmetric unit. Refinement of the population of each of these fragments resulted in near equivalent values of 0.25. For compounds **3** and **6**, the two Cp orientations had equal populations. In addition, one disordered half-molecule of hexane is present in the asymmetric unit of **6**. This disorder was modeled in two orientations, with restraints employed to maintain similar geometries. Compound **8** crystallizes with two independent molecules in the asymmetric unit. Compound **9** crystallizes as a two-component split crystal with the two components related by a 51° rotation about the (0 0 1) real axis. Data were integrated for both twin components, including both overlapping and non-overlapping reflections. The structure was solved using non-overlapped data from the major twin component. Subsequent refinements of **9** were carried out using HKLF 5 format data set containing complete from component 2 and all overlapped reflections from component 1. The batch scale refinement showed a roughly 53:47 ratio between the major and minor twin components. All non-hydrogen atoms (except those of the Cp ring for compound **2** and the disorder solvent atoms for **6**) were refined anisotropically. All hydrogen atoms were placed in calculated positions but were not refined. All refinements were performed using the SHELXTL crystallographic software package of Bruker-AXS.³⁶ The molecular drawings were generated by the use of ORTEP-3³⁷ and POV-Ray. Crystal data and structure refinement parameters are collected in the Supporting Information.

Computational Details. QM/MM calculations were carried out by use of the Gaussian03 suite of programs³⁸ with use of the B3LYP functional³⁹ within the DFT methodology for the QM part and the UFF⁴⁰ for the MM part. The basis set chosen for the QM calculations comprised the 6-31G* set for the C, N, and O atoms, the 6-31G** set for the H atoms, and the SDD set, which includes a pseudopotential, augmented by an f polarization function with the optimized⁴¹ 1.941 coefficient for the Cr atom. The cutoff between the QM and MM parts was placed at the level of the Ar–N bonds, with the N=C(Me)–CH–C(Me)=N diketiminato moiety being treated quantummechanically together with the Cr atom, the Cp ring, and the CH(OAc)CH₃ ligand, while the entire aryl substituents were handled at the MM level. The input geometries were obtained or adapted from the crystallographically characterized compounds. Spin contamination was negligible, all calculations

(33) SAINT, version 7.03A; Bruker Analytical X-ray System: Madison, WI, 1997–2003.

(34) SADABS, Bruker Nonius area detector scaling and absorption correction, V2.10; Bruker AXS Inc.: Madison, Wisconsin, 2003.

(35) Altomare, A.; Burla, M.; Camalli, M.; Cascarano, G.; Giacovazzo, C.; Guagliardi, A.; Moliterni, A.; Polidori, G.; Spagna, R. *J. Appl. Crystallogr.* **1999**, *32*, 115–119.

(36) Sheldrick, G. M. *SHELXTL*, version 5.1; Bruker AXS, Inc.: Madison WI, 1997.

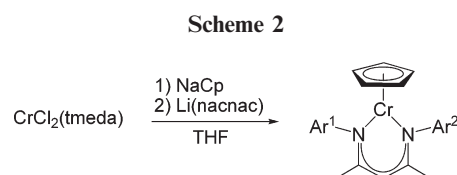
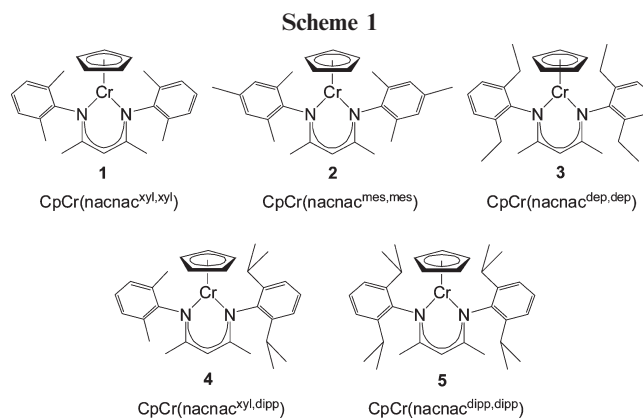
(37) Farrugia, L. J. *J. Appl. Crystallogr.* **1997**, *32*, 565.

(38) Frisch, M. J.; et al. *Gaussian 03, Revision D.01*; Gaussian, Inc.: Wallingford, CT, 2004.

(39) Becke, A. D. *J. Chem. Phys.* **1993**, *98*, 5648–5652.

(40) Rappe, A. K.; Casewit, C. J.; Colwell, K. S.; Goddard, W. A.; Skiff, W. M. *J. Am. Chem. Soc.* **1992**, *114*, 10024–10035.

(41) Ehlers, A. W.; Boehme, M.; Dapprich, S.; Gobbi, A.; Hoellwarth, A.; Jonas, V.; Koehler, K. F.; Stegmann, R.; Veldkamp, A.; Frenking, G. *Chem. Phys. Lett.* **1993**, *208*, 111–114.



converging with $\langle S^2 \rangle$ close to the expected values (6 for the quintet state of Cr^{II}, 6.022 for all three compounds; 3.75 for the quartet state of Cr^{III}, 3.824 for the Dipp derivative). The values reported are the electronic energies without ZPVE correction.

Results and Discussion

a. Syntheses and Characterization of CpCr^{II}(nacnac). The CpCr^{II}(nacnac) compounds used in this study are shown in Scheme 1 (xyl = 2,6-dimethylphenyl; mes = 2,4,6-trimethylphenyl; dep = 2,6-diethylphenyl; dipp = 2,6-diisopropylphenyl). Of these, only compounds **1**¹⁶ and **5**^{14,16} have previously been described in the literature.

The new CpCr^{II}(nacnac) complexes **2–4** were prepared following the literature procedure reported for **1**,^{14,16} which consists of the one-pot reaction of CrCl₂(tmeda) with 1 equiv of NaCp, followed by 1 equiv of the appropriate nacnacLi salt (Scheme 2). Compounds **1–5** are highly air sensitive. The ¹H NMR spectra of compounds **2–4** in C₆D₆ all displayed multiple broad, overlapping, unassignable signals between 0 and 13 ppm. The magnetic susceptibilities of complexes **2–4** were determined using the Evans method³² and were consistent with the high-spin Cr^{II} configuration previously determined for **1**.¹⁴ As previously reported for compound **5**,¹⁴ solutions of the Cr^{II} complexes **1–4** are green to incident light with a distinctive magenta color to transmitted light. They exhibit two very strong bands at 307–308 and 427–430 nm, comparable to those observed for three-coordinate Cr^{II} nacnac alkyl complexes.⁴² Compounds **1–5** also have a less intense single band at 558–576 nm.

Compounds **2** and **3** have also been characterized by single-crystal X-ray diffraction. The geometry of the two Cr^{II} compounds (Figure 1) can be described as a “two-legged piano stool”, with the Cp ring centroid lying close to the plane defined by the Cr1, N1, and N2 or N1* atoms. Relevant bond distances and angles are collected in Table 1. The bonding parameters for compounds **2** and **3** are very similar to those found in previously reported structures for CpCr(nacnac) Cr^{II} complexes.^{14,16}

(42) Fan, H. J.; Adhikari, D.; Saleh, A. A.; Clark, R. L.; Zuno-Cruz, F. J.; Cabrera, G. S.; Huffman, J. C.; Pink, M.; Mendiola, D. J.; Baik, M. H. *J. Am. Chem. Soc.* **2008**, *130*, 17351–17361.

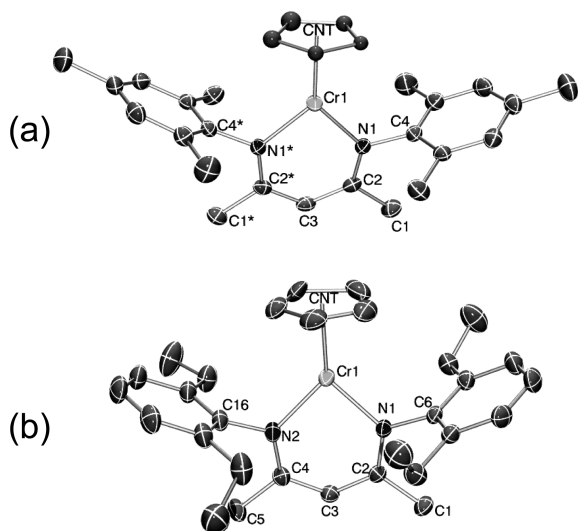


Figure 1. Views of compounds **2** (a) and **3** (b), with thermal ellipsoids drawn at the 50% probability level. All H atoms are omitted and only one Cp orientation is shown for clarity.

Table 1. Selected Bond Distances (Å) and Angles (deg) for Compounds **2** and **3**

	2	3
Distances		
CNT–Cr	2.00(1)	2.013(12)
Cr–N	2.007(2)	2.0276(12)
Cr–N		2.0260(12)
Angles		
CNT–Cr–N	134.0(3)	134.8(3)
CNT–Cr–N		134.5(3)
CNT–(CrN ₂) ^a	177.7(3)	173.8(3)
N–Cr–N	91.2(1)	90.37(5)

^a Angle between the CNT–Cr vector and the CrN₂ plane

b. VAc Polymerizations under OMRP: V-70 Initiator.

Before presenting the new results, it is necessary to review those already described in a recent communication.¹⁶ Compound **1** was shown to trap radicals produced by V-70 in the presence of VAc, since a polymerization test with VAc/V-70/**1** = 500:0.8:1 at 50 °C for 4 h and then at 90 °C gave only an 11% monomer conversion after 8 h ($M_{n,SEC} = 11\,500$ vs the expected value of 4730, $M_w/M_n = 1.81$), which no longer increased upon warming at 90 °C for 66 h. Conversely, compound **5** gave a much higher monomer conversion, since a polymerization with VAc/V-70/**5** = 500:0.8:1 gave a linearly growing M_n up to a conversion of 70% ($M_{n,SEC} = 67\,300$ vs the expected value of 30 100, $M_w/M_n = 1.80$) in 46 h under much milder conditions ($T = 30$ °C). Although the controlling ability was poor (low initiator efficiency, high polydispersity), the sustained polymerization and the M_n growth with conversion demonstrated the reversibility of radical trapping. The hypothesis that both complexes operate with formation of an organometallic dormant chain, Cp(nacnac^{Ar,Ar})Cr^{III}–PVAc, with a much weaker Cr^{III}–PVAc bond when Ar = dipp (compound **5**) relative to Ar = xyl (compound **1**) seemed fully consistent with DFT calculations of the bond strengths. The larger system with Ar = dipp was not calculated, but a comparison of the bond dissociation energy for the two related systems with Ar = xyl

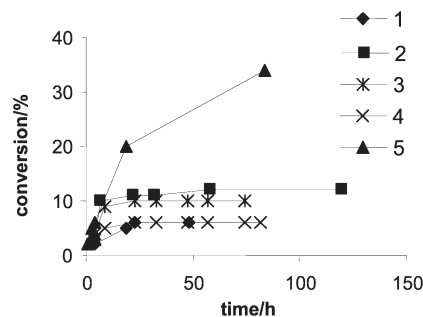


Figure 2. Conversion as a function of time for the VAc polymerization initiated by V-70 in the presence of compounds **1–5**. Conditions: VAc/V-70/Cr^{III} = 500:0.8:1. $T = 50$ °C for 4 h, then 90 °C.

and Ph (19.7 and 28.4 kcal mol⁻¹ at the B3LYP/6-31G* level, respectively) indicated a strong effect of the steric congestion created by the aryl substituents on the ability of the organometallic dormant chain to release free radicals in solution.

We now report subsequent studies with compounds **1** and **5**, as well as with compounds **2–4**, which revealed a more complex and interesting state of affairs. Compounds **2–4** were synthesized with the idea of fine controlling the Cr^{III}–PVAc BDE, thus allowing the development of a system capable of yielding a suitable polymerization rate and degree of control. However, a steric bulk increase on going from **1** to **2** and then to **3** and **4** did not produce any significant labilization of the Cr^{III}–PVAc bond since the polymerization did not proceed in any of these cases beyond 12% conversion for experiments carried out at 90 °C; see Figure 2. Indeed, the polymerization essentially stops in each case after an initial burst of monomer consumption, within the first 5–10 h.

On the other hand, new polymerization experiments with compound **5**, run at higher temperatures, gave a lower apparent polymerization rate constant, only 34% conversion after 84 h at 90 °C. The M_n value increased linearly with conversion and the M_w/M_n decreased to reach a value of only 1.21 for the final sample (see Figure 3), although the M_n was much greater than expected (54 800 vs 14 600). A polymerization process that takes place rapidly under mild conditions (30 °C)¹⁶ cannot become slower at a higher temperature while maintaining the same mechanism. It is more logical to think of a deactivation process (*vide infra*).

c. Design of a Single-Component Chromium Reagent as OMRP Initiator. Well-defined Cr^{III}–R complexes could serve as single-component OMRP reagents if they possessed a Cr–alkyl bond that was sufficiently weakened by steric interactions to readily undergo homolysis.^{12,13} To date, the success of synthetic routes to CpCr(nacnac)X complexes has depended on the degree of steric bulk in the target molecule. For the 2,6-*i*Pr₂-substituted system, CpCr(nacnac^{dipp,dipp})Cl was difficult to prepare by salt metathesis and did not react cleanly with Grignard reagents.¹⁴ In contrast, reducing the size of the *ortho* substituents in the nacnac ligands was found to greatly improve both the synthesis and salt metathesis reactivity.^{15,43} For example, CpCr(nacnac^{xyl,xyl})Me was readily prepared from CpCr(nacnac^{xyl,xyl})Cl with MeMgI.¹⁵ Synthesis of the corresponding CpCr(nacnac^{dipp,dipp})Me had necessitated the use of the corresponding Cr^{III} triflate complex.¹⁴

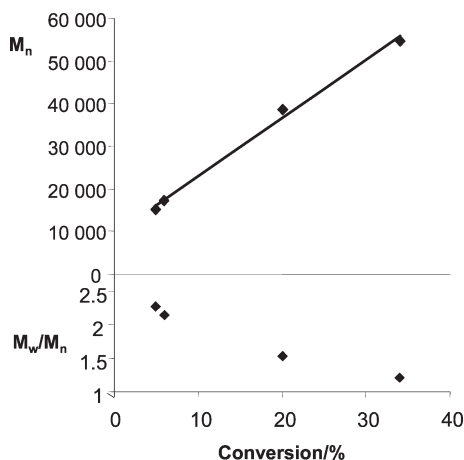


Figure 3. Number average molecular weight and polydispersity index for the PVAc obtained in the presence of compound 5. Conditions are as in Figure 2.

Isolated $\text{CpCr}(\text{nacnac}^{\text{xy1,xy1}})\text{Me}$ does not serve as an effective single-component OMRP reagent. When 16.1 mg of this Cr^{III} methyl complex was dissolved in 4 mL of neat vinyl acetate, only a 9% mass conversion was observed after 48 h at room temperature. The resulting polymer had both a high M_n (83 900 compared to 9140 expected M_n) and a high PDI of 3.4. The lack of steric pressure on the small methyl ligand and the relative instability of the $\text{CH}_3\cdot$ radical should make the $\text{Cr}^{\text{III}}\text{--CH}_3$ BDE high and the homolytic dissociation unfavorable. Initiation to form $\text{CH}_3\cdot$ and the Cr^{II} radical trap will thus be inefficient at room temperature. However, the observation of a small amount of uncontrolled polymerization leading to high M_n is consistent with the slow release of $\text{CH}_3\cdot$ radicals, which then react rapidly in neat vinyl acetate.⁴⁴

For an efficient single-component OMRP reagent, a Cr^{III} alkyl complex is required that has a low $\text{Cr}\text{--R}$ BDE and that generates a $\text{R}\cdot$ radical capable of reacting rapidly with vinyl acetate. The steric pressure exerted by the neopentyl ligand has often been used to encourage not only intramolecular deprotonation reactions^{17–20} but also metal–alkyl bond homolysis.^{21–23} While several classes of even-electron monomeric chromium neopentyl complexes are known for Cr^{II} ,^{31,45} Cr^{IV} ,^{46,47} and Cr^{VI} ,^{48–50} well-defined Cr^{III} neopentyl complexes are relatively unexplored.⁵¹

(44) Solution phase measurements give the bimolecular rate constant for the reaction of methyl radical with vinyl acetate as $1.4 \times 10^4 \text{ M}^{-1} \text{ s}^{-1}$, while the same reaction with the more stabilized benzyl radical has $k = 14 \text{ M}^{-1} \text{ s}^{-1}$: (a) Zytowski, T.; Fischer, H. *J. Am. Chem. Soc.* **1996**, *118*, 437–439. (b) Fischer, H.; Radom, L. *Angew. Chem., Int. Ed.* **2001**, *40*, 1340–1371.

(45) Hermes, A. R.; Morris, R. J.; Girolami, G. S. *Organometallics* **1988**, *7*, 2372–2379.

(46) Mowat, W.; Shortland, A. J.; Hill, N. J.; Wilkinson, G. *J. Chem. Soc., Dalton Trans.* **1973**, 770–778.

(47) Schulzke, C.; Enright, D.; Sugiyama, H.; LeBlanc, G.; Gambarotta, S.; Yap, G. P. A.; Thompson, L. K.; Wilson, D. R.; Duchateau, R. *Organometallics* **2002**, *21*, 3810–3816.

(48) Meijboom, N.; Schaverien, C. J.; Orpen, A. G. *Organometallics* **1990**, *9*, 774–782.

(49) Danopoulos, A. A.; Wilkinson, G.; Sweet, T. K. N.; Hursthouse, M. B. *J. Chem. Soc., Dalton Trans.* **1995**, 2111–2123.

(50) Coles, M. P.; Gibson, V. C.; Clegg, W.; Elsegood, M. R. J.; Porrelli, P. A. *J. Chem. Soc., Chem. Commun.* **1996**, 1963–1964.

(51) The metallocyclobutane $\text{Cp}^*\text{Cr}(\text{pyridine})(\text{CH}_2)_2\text{CMe}_2$ has been prepared via the route developed for the analogous CH_2SiMe_3 reactions: Heintz, R. A.; Leelasubcharoen, S.; Liable-Sands, L. M.; Rheingold, A. L.; Theopold, K. H. *Organometallics* **1998**, *17*, 5477–5485.

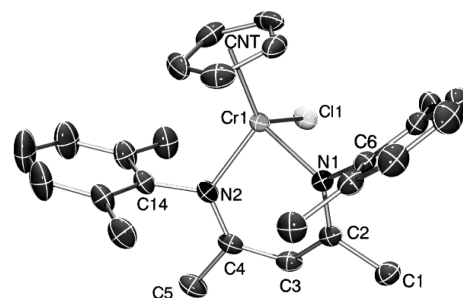


Figure 4. Thermal ellipsoid diagram (50%) of compound 6. All H atoms are omitted and only one Cp orientation is shown for clarity. Selected bond lengths (Å): $\text{Cr}(1)\text{--N}(1)$, 2.018(2); $\text{Cr}(1)\text{--N}(2)$, 2.020(2); $\text{Cr}(1)\text{--CNT}$, 1.92(2); $\text{Cr}(1)\text{--Cl}(1)$, 2.3082(5). Selected bond angles (deg): $\text{N}(1)\text{--Cr}(1)\text{--N}(2)$, 90.47(7); $\text{N}(1)\text{--Cr}(1)\text{--Cl}(1)$, 94.28(5); $\text{N}(2)\text{--Cr}(1)\text{--Cl}(1)$, 93.14(5); $\text{CNT}\text{--Cr}(1)\text{--N}(1)$, 124.8(4); $\text{CNT}\text{--Cr}(1)\text{--N}(2)$, 125.0(4); $\text{CNT}\text{--Cr}(1)\text{--Cl}(1)$, 120.34(6); $\text{CNT}\text{--}(\text{CrN}_2)^a$, 160.5(4). ^aAngle between the $\text{CNT}\text{--Cr}$ vector and the CrN_2 plane.

The synthesis of compound $\text{CpCr}(\text{nacnac}^{\text{xy1,xy1}})\text{Cl}$ (**6**) was achieved by reacting CrCl_3 with 1 equiv of $\text{Li}(\text{nacnac}^{\text{xy1,xy1}})$, followed by 1 equiv of NaCp to yield an air-stable crystalline solid. The geometry of **6** (Figure 4) can be described as a “three-legged piano stool” and is ubiquitous of half-sandwich Cr^{III} complexes. The $\text{Cr}\text{--Cl}$ bond length of 2.3082(5) Å is similar to that found in $\text{CpCr}(\text{nacnac}^{\text{dipp,dipp}})\text{Cl}$,¹⁴ as well as other cyclopentadienyl Cr^{III} complexes with terminal Cl groups, such as $\text{CpCr}(\text{acac})\text{Cl}$ and $\text{Cp}^*\text{Cr}(\text{acac})\text{Cl}$ ($\text{Cr}\text{--Cl}$ of 2.299(1) and 2.307(1) Å, respectively).⁵² It is also similar to the $\text{Cr}\text{--Cl}$ distance in six-coordinate Cr^{III} *nacnac* complexes with terminal Cl ligands (2.346(1) Å for $\text{Cr}(\text{nacnac}^{\text{Ph,Ph}})\text{Cl}_2\text{--}(\text{THF})$ ⁵³ and 2.2947(12) Å for $\text{Cr}(\text{nacnac}^{\text{dipp,dipp}})(\text{O}_2\text{CMe})\text{Cl}(\text{THF})$ ⁵⁴), while five-coordinate Cr^{III} *nacnac* complexes display shorter $\text{Cr}\text{--Cl}$ bond lengths (2.233(2) and 2.2294(14) Å for the terminal chloride ligands in $[\text{Cr}(\text{nacnac}^{\text{dipp,dipp}})\text{Cl}(\mu\text{-Cl})]_2$ and $\text{Cr}(\text{nacnac}^{\text{dipp,dipp}})[(\text{OCPh})_2\text{CH}]\text{Cl}$, respectively).⁵⁴ Unlike the geometries of **2** and **3**, the Cr atom deviates significantly from the plane of the *nacnac* ligand, toward the Cl atom. The Cr in **6** lies 0.615(3) Å out of the imaginary plane defined by the $\text{N1}\text{--C2}\text{--C4}\text{--N2}$ atoms, which is smaller than the 0.72 Å out-of-plane distortion previously observed for the bulkier $\text{CpCr}(\text{nacnac}^{\text{dipp,dipp}})\text{Cl}$.¹⁴ Relative to the Cr^{II} structures, the $\text{Cr}\text{--CNT}$ distance is slightly shorter, whereas the $\text{Cr}\text{--N}$ distances are not significantly different.

While **6** is a useful precursor to $\text{CpCr}(\text{nacnac}^{\text{xy1,xy1}})\text{Me}$,¹⁵ attempts to install more sterically demanding alkyl ligands once again required the use of a better leaving group. The reaction of compound **6** with 1 equiv of AgOTf provides compound **7** in high yields as an air-stable crystalline solid (Figure 5). Preliminary reactions between **6** and AgOTf or AgOTf had indicated that the Cr^{III} tosylate was less air sensitive and more crystalline than the Cr^{III} triflate complex. The $\text{Cr}\text{--O}$ bond length in **7**, 1.9839(15) Å, is slightly shorter than the 2.030(1) observed for the $\text{CpCr}(\text{nacnac}^{\text{dipp,dipp}})\text{--}(\text{OTf})$,¹⁴ which may be attributable to the lower electron-withdrawing power of the *para*-tolyl substituent compared

(52) Heinemann, O.; Jolly, P. W.; Krüger, C.; Verhovnik, G. P. *J. Organomet. Chem.* **1998**, *553*, 477–479.

(53) Kim, W.-K.; Fevola, M. J.; Liable-Sands, L. M.; Rheingold, A. L.; Theopold, K. H. *Organometallics* **1998**, *17*, 4541–4543.

(54) Gibson, V. C.; Newton, C.; Redshaw, C.; Solan, G. A.; White, A. J. P.; Williams, D. J. *Eur. J. Inorg. Chem.* **2001**, 1895–1903.

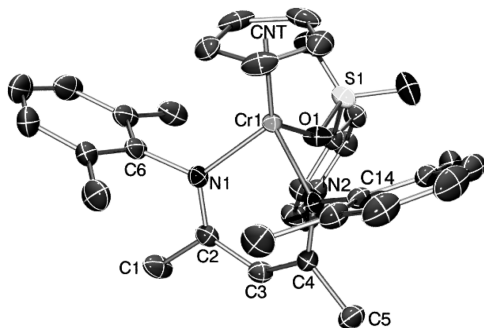


Figure 5. Thermal ellipsoid diagram (50%) of compound **7**. All H atoms are omitted for clarity. Selected bond lengths (Å): Cr(1)–N(1), 2.0038(16); Cr(1)–N(2), 2.0019(17); Cr(1)–C(NT), 1.896; Cr(1)–O(1), 1.9839(15). Selected bond angles (deg): N(1)–Cr(1)–N(2), 90.17(7); N(1)–Cr(1)–O(1), 91.45(7); N(2)–Cr(1)–O(1), 92.48(7); CNT–Cr(1)–N(1), 125.74; CNT–Cr(1)–N(2), 123.82; CNT–Cr(1)–O(1), 123.32; Cr(1)–O(1)–S(1), 135.77(9).

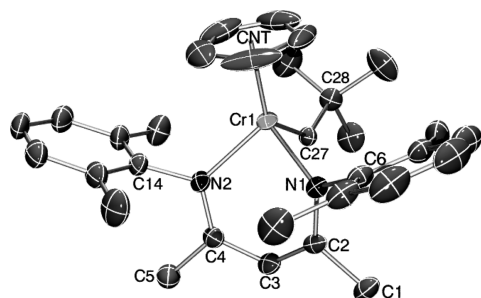


Figure 6. Thermal ellipsoid diagram (50%) of compound **8**. Compound **8** has two independent molecules in the crystal lattice; only one is shown and all H atoms are omitted for clarity. Selected bond lengths (Å): Cr(1)–N(1), 2.046(2); Cr(1)–N(2), 2.051(2); Cr(1)–C(NT), 1.949; Cr(1)–C(27), 2.136(3). Selected bond angles (deg): N(1)–Cr(1)–N(2), 89.71(9); N(1)–Cr(1)–C(27), 93.50(10); N(2)–Cr(1)–C(27), 93.63(10); CNT–Cr(1)–N(1), 123.03; CNT–Cr(1)–N(2), 122.29; CNT–Cr(1)–C(27), 125.39; Cr(1)–C(27)–C(28), 135.1(2).

to CF₃, the decreased steric demand of the 2,6-Me₂C₆H₃-substituted nacnac, or both.

The reaction of compound **7** with 0.5 equiv of Mg-(CH₂CMe₃)₂·1.05(1,4-dioxane) gave CpCr(nacnac^{xy1,xy1})Np (**8**), where Np = neopentyl, CH₂CMe₃. The use of the halide-free dialkyl Mg reagent was required to avoid unwanted substitution of the tosylate ligand in **7** with a halide prior to alkylation to form **8**. Complex **8** was found to be highly soluble in nonpolar solvents, similar to the previously reported CpCr(nacnac^{xy1,xy1})Me.^{14,15} The structural characterization of **8** has been achieved by single-crystal X-ray diffraction (Figure 6). The Cr–C(27) bond is significantly elongated in **8** (2.136(3) Å) compared to the 2.076(2) Å observed previously for the corresponding Cr^{III} methyl complex.¹⁵ The Cr–N bond lengths in **8** are also slightly longer, and the Cr–C(27)–C(28) angle is 135.1(2)°, indicative of the strain imposed by the *t*Bu substituent of the neopentyl ligand. Solutions of **8** are purple, exhibiting strong bands in the UV–visible spectrum at 404 and 567 nm. The strong absorbance around 550 nm seems characteristic of CpCr(nacnac)(alkyl) complexes: the increase in absorbance at 530 nm due to formation of CpCr(nacnac)Me was used to

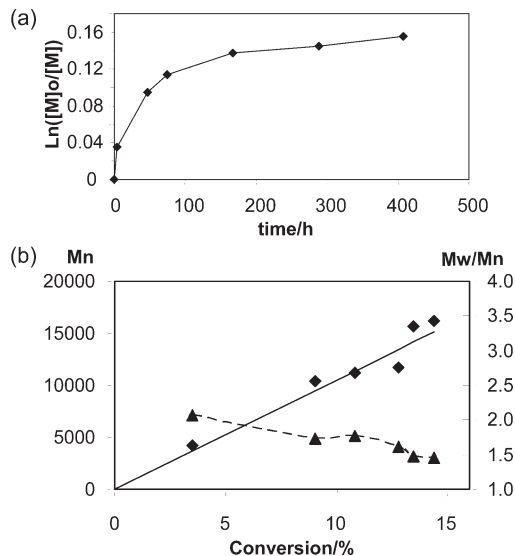


Figure 7. (a) $\ln([VAc]_0/[VAc])$ as a function of time for the VAc polymerization initiated by compound **8**. Conditions: VAc/**8** = 1200:1. T = room temp. (b) Variation of the $M_{n,SEC}$ (diamonds) and M_w/M_n (triangles) as a function of conversion; the solid line represents $M_{n,th}$.

monitor the kinetics of iodomethane activation with CpCr(nacnac) complexes **1**–**3**.¹⁵ Although **8** was stable in solution to allow for recrystallization from hexanes, decomposition took place upon dilution (necessary for UV/vis characterization) to yield CpCr(nacnac^{xy1,xy1}), **1**. The decrease in stability of **8** at high dilution is consistent with the facile homolytic Cr–C bond cleavage, paralleling the reactivity of other neopentyl complexes,^{21–23} with formation of compound **1** and an extremely reactive neopentyl radical, and indicated the potential for complex **8** to be used as a single-component reagent to initiate and control the radical polymerization of vinyl acetate.

d. OMRP of VAc with Complex 8. Polymerizations of VAc in the presence of complex **8** (VAc/**8** = 1200:1) at room temperature gave a linearly growing M_n up to a monomer conversion of 14% after 400 h ($M_{n,SEC} = 16\,200$ vs the expected value of 15 100, $M_w/M_n = 1.46$); see Figure 7. These results contrast with the uncontrolled polymerization observed with CpCr(nacnac^{xy1,xy1})Me under the same conditions as discussed above. There is no visible induction period, and the good agreement between the observed and calculated M_n demonstrates the increased initiator efficiency compared with the OMRP reactions with the V-70 initiator. However, the progressive decrease of the polymerization rate constant (decreasing slope in Figure 7a) suggests that partial deactivation of the growing chains occurs, which also causes the broad molecular weight distribution.

Spectroscopic analysis of the polymerization reaction of vinyl acetate with **8** revealed absorbance peaks at 422 and 556 nm, at a reaction time of 10 min, indicating that **8** had been completely consumed, presumably being transformed into the CpCr(nacnac^{xy1,xy1})(PVAc) dormant species. This is again in contrast to the previously discussed reaction of CpCr(nacnac^{xy1,xy1})Me in vinyl acetate, where after 48 h the absorbance peak of the Cr^{III} methyl starting material was still evident at 546 nm. Throughout the progress of the polymerization reaction initiated by **8**, the UV/vis spectrum further evolved to yield a shift of the major band toward

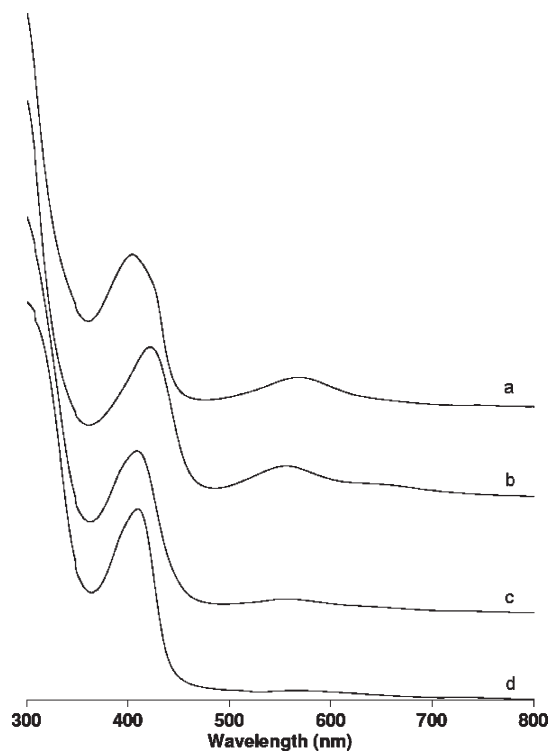


Figure 8. Evolution of the UV/vis properties during the VAC polymerization controlled by compound **8** (conditions as shown in Figure 7). (a) Initial spectrum of compound **8**; (b) after 10 min of polymerization; (c) after 400 h of polymerization; (d) after warming to 70 °C (spectrum of the decomposition product).

higher frequency (412 nm), while the 556 nm band decreased in intensity; see Figure 8. This spectral evolution parallels the observed decrease in polymerization rate (Figure 7). After 400 h of polymerization process, the sample was heated at 70 °C for 3.5 h to produce a color change from purple to green (incident light) and orange (transmitted light) with the higher energy absorption band increasing in intensity and the 556 nm band disappearing and being replaced by a less intense band at 575 nm. The results suggested that, even though the rate of polymerization had slowed significantly (see Figure 7), there was still some $\text{CpCr}^{\text{III}}(\text{nacnac}^{\text{xyl,xyl}})(\text{PVAc})$ compound present after 400 h of polymerization, which underwent further reactivity once heated.

It is striking to compare the behavior of the polymerization initiated by compound **8** on one side (14% in 400 h at room temperature, Figure 7) with that initiated by the **1/V-70** mixture (5% in 50 h at 90 °C, Figure 2), both leading in principle to the same OMRP equilibrium. This clearly proves that the $\text{CpCr}^{\text{III}}(\text{nacnac}^{\text{xyl,xyl}})(\text{PVAc})$ dormant chain can be reversibly reactivated under mild conditions to sustain the OMRP of vinyl acetate, but it also suffers irreversible thermal deactivation, even at room temperature at a slow rate and much faster at more elevated temperatures.

It is interesting to compare the relatively slow polymer growth in the presence of the $\text{CpCr}(\text{nacnac}^{\text{xyl,xyl}})$ system and the previously reported¹⁶ faster polymer growth in the presence of the $\text{CpCr}(\text{nacnac}^{\text{dipp,dipp}})$ system (70% conversion in 46 h at 30 °C). This difference confirms the previously proposed steric effect on the homolytic bond dissociation energy, which is further investigated at the theoretical level in the next section.

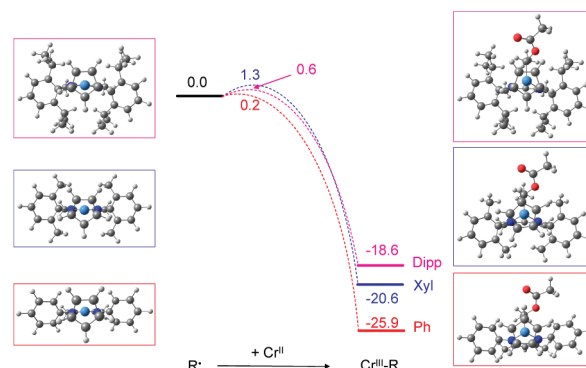


Figure 9. Optimized geometries and QM/MM relative energies (in kcal/mol) of geometry-optimized $\text{CpCr}^{\text{II}}(\text{nacnac}^{\text{Ar,Ar}})$ and $\text{CpCr}^{\text{III}}(\text{nacnac}^{\text{Ar,Ar}})(\text{CHMeOOCMe})$ for Ar = Ph, Xyl, and Dipp.

e. DFT Study of the OMRP Trapping Processes. The previous communication reported geometry optimizations at the full QM level using density functional theory (DFT) for $\text{CpCr}^{\text{II}}(\text{nacnac}^{\text{Ar,Ar}})$ and $\text{CpCr}^{\text{III}}(\text{nacnac}^{\text{Ar,Ar}})(\text{CHMeOOCMe})$ (a model of the OMRP dormant chain), leading to the calculation of the $\text{Cr}^{\text{III}}-\text{C}$ BDE values of 28.4 and 19.7 kcal/mol for Ar = Ph and Xyl, respectively.¹⁶ This shows a tremendous steric effect of the nacnac aryl substituents on the $\text{Cr}^{\text{III}}-\text{C}$ bond fragility, which is also reflected in the optimized $\text{Cr}^{\text{III}}-\text{C}$ distances (2.109 and 2.124 Å, respectively). Calculations of the Ar = dipp system were not carried out because they are too time-consuming at the full QM level. We now report QM/MM results for the same systems as well as for the bulkier dipp system in terms of both energetics and radical-trapping barriers. The energetic results and views of the optimized structures are shown in Figure 9, whereas the essential bonding parameters are given in Table 2. All optimized geometries are available in the Supporting Information in the form of Cartesian coordinates. The calculations were carried out with imposition of the experimentally determined spin state ($S = 3/2$ for the alkylchromium(III) complexes and $S = 2$ for the chromium(II)-trapping species), leading to calculated structures in excellent agreement with those determined crystallographically for complexes **1** and **5**. The calculated $\text{Cr}-\text{C}$ bond lengths for the cyclopentadienyl ligand are longer than those observed experimentally:⁵⁵ the $\text{CNT}-\text{Cr}$ distances for the Cr^{II} Xyl and Dipp nacnac complexes were 2.022 and 2.016 Å for **1** and **5**, respectively.

The energetic results in terms of $\text{BDE}(\text{Cr}^{\text{III}}-\text{C})$ for the Ph and Xyl systems are quite close to those previously obtained at the full QM level, although the steric labilization exerted by the four Me groups is predicted as less severe by the QM/MM calculations relative to the full QM level. The present calculation uses a polarized SDD basis set for the Cr atom, which is considered as more balanced than the LANL2DZ basis set without polarization functions previously used in the full QM calculations.¹⁶ The presence of a steric effect is confirmed on going from the Xyl to the Dipp substituents, where the four *i*Pr groups induce a further $\text{Cr}^{\text{III}}-\text{C}$ bond labilization by 2.0 kcal/mol relative to four Me groups. This labilization is accompanied by a significant lengthening of the $\text{Cr}^{\text{III}}-\text{C}$ bond, in the order Ph (2.091 Å) < Xyl (2.115 Å) < Dipp (2.139 Å).

(55) Gallant, A. J.; Smith, K. M.; Patrick, B. O. *Chem. Commun.* **2002**, 2914–2915.

Table 2. Selected Bond Distances (Å) and Angles (deg) for the B3LYP//UFF Optimized Geometries

complex	CpCr ^{II} (nacnac ^{Ar,Ar})			TS			CpCr ^{III} (nacnac ^{Ar,Ar})(R) ^a			
	Ar	Ph	Xyl	Dipp	Ph	Xyl	Dipp	Ph	Xyl	Dipp
Distances										
CNT–Cr	2.081	2.081	2.070	2.072	2.080	2.079	2.070	2.081	2.096	
Cr–N	2.014	2.009	2.028	2.021	2.024	2.051	2.018	2.033	2.062	
	2.014	2.009	2.030	2.020	2.021	2.040	2.024	2.034	2.088	
Cr–C				4.290	3.440	3.396	2.091	2.115	2.139	
Angles										
CNT–Cr–N	133.3	133.6	132.3	134.2	131.7	131.9	121.6	123.5	123.8	
	133.2	133.6	133.9	133.3	131.0	132.1	124.4	124.5	124.5	
CNT–Cr–C				108.7	106.0	101.4	117.6	114.9	114.1	
CNT–(CrN ₂) ^b	175.8	179.5	178.5	178.6	161.4	167.5	141.8	143.3	143.7	
N–Cr–N	93.3	92.7	93.8	92.4	91.6	93.4	92.3	90.1	91.7	
N–Cr–C				77.5	92.2	92.3	97.5	100.2	102.0	
				75.1	91.4	89.1	97.2	97.8	94.8	

^a R = CHMeOOCMe. ^b Angle between the CNT–Cr vector and the CrN₂ plane.

We have also optimized the transition state leading from the CpCr^{II}(nacnac^{Ar,Ar}) complex plus free radical to the OMRP dormant species. The coordination geometry is quite close to that of the Cr^{II} complex with a rather long Cr^{II}–C distance; that is, the transition state is early for the radical-trapping process, consistent with the very low calculated energy barrier. The barrier is lowest, as expected, for the less encumbered Ph derivative, whereas the most encumbered Dipp system yields a lower barrier than the Xyl system with intermediate steric demand. Although the barrier for trapping the radical is very low for all three systems, the unexpectedly lower barrier for the Dipp derivative may be attributable to the structure of the Cr^{II} complex. The calculated ground-state structure of CpCr(nacnac^{dipp,dipp}) faithfully reproduces the slight bowing of the N-aryl substituents out of the plane defined by the nacnac ligand that was observed in the X-ray structure of **1**.¹⁴ As suggested by a helpful reviewer, this sterically induced initial deformation of the Cr^{II} Dipp complex may permit a slightly lower energy approach of the alkyl radical compared to CpCr(nacnac^{xyl,xyl}), which does not display this distortion.

f. Isolation of the Deactivated Complex. As discussed above, UV–vis analysis of the Cr^{III} neopentyl compound in vinyl acetate suggested that while **8** was consumed within minutes at room temperature, a subsequent thermal decomposition reaction occurred and that this is accelerated by heating. To determine the ultimate fate of the organochromium complex, the thermolyzed reaction mixture of 35.8 mg of **8** in 4 mL of vinyl acetate was evacuated and the unknown Cr species was extracted from the PVAc with diethyl ether. After filtration, concentration, and storage at –35 °C for two weeks, 7.9 mg of X-ray quality crystals of CpCr(nacnac^{xyl,xyl})-OC(O)Me (**9**) (Figure 10) was obtained, corresponding to a 23% isolated yield based on **8**.

The independent synthesis of **9** was achieved by the reaction of **6** with 1 equiv of AgOAc, with UV–visible spectroscopic analysis confirming that **9** was the thermal decomposition product of the polymerization reaction. Upon reexamination of the V-70-initiated OMRP experiments, UV–vis spectroscopy confirmed that the Cr^{III} acetate complex was a common termination pathway for all of the Cr-mediated vinyl acetate polymerization reactions conducted at elevated temperatures. Suspicions arose about the possibility of Cr^{III} acetate formation by oxidative addition of a =CH–OC(O)CH₃ moiety from the polymer chain. However, a control experiment showed no signs of reactivity

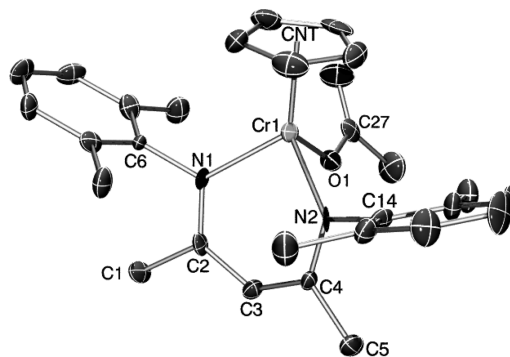
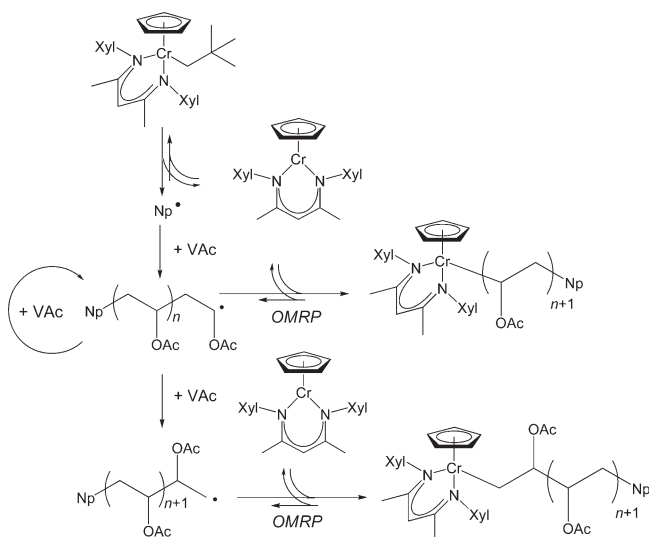


Figure 10. Thermal ellipsoid diagram (50%) of **9**. All H atoms are omitted for clarity. Selected bond lengths (Å): Cr(1)–N(1), 2.010(5); Cr(1)–N(2), 2.004(6); Cr(1)–CNT, 1.914; Cr(1)–O(1), 1.952(5); C(27)–O(1), 1.278(9); C(27)–O(2), 1.230(9). Selected bond angles (deg): N(1)–Cr(1)–N(2), 90.7(2); N(1)–Cr(1)–O(1), 92.7(2); N(2)–Cr(1)–O(1), 88.6(2); CNT–Cr(1)–N(1), 124.94; CNT–Cr(1)–N(2), 123.34; CNT–Cr(1)–O(1), 125.92; Cr(1)–O(1)–C(27), 133.6(5).

for compound **1** toward commercially obtained PVAc upon heating to 50 °C for 24 h. Similarly, prolonged heating of **1** in vinyl acetate does not result in any change in the UV/vis spectrum of **1**. These results suggested a more complicated mechanism for the formation of CpCr(nacnac)OAc. The proposed mechanism for the formation of **9** is that of β -acetate elimination arising from a 2,1-insertion (head-to-head) of the monomer, as shown in Scheme 3. Head-to-head insertion is known to be particularly problematic for the radical polymerization of vinyl acetate, due to the relatively poor regioselectivity of radical addition.^{1,5} Note that the 2,1-insertion step may lead to the generation of a dormant species with a presumably stronger Cr^{III}–C bond, which could also contribute to a gradual slow down of the polymerization process.

Elimination of β -acetate groups has been well documented as a decomposition mode in attempts to copolymerize ethylene and vinyl acetate with Ni and Pd catalysts.^{2,3} We point out, however, that the β -acetate elimination process from the newly formed dormant species is not likely to follow a classical β -elimination mechanism, because this requires an open coordination site on Cr capable of accepting the two additional electrons furnished by the incoming acetate group. While the metal is electronically unsaturated (15 electrons) and metal-based orbitals are indeed available, the latter are however

Scheme 3



half-occupied because of the ubiquitous spin quartet configuration of half-sandwich Cr^{III}. Expansion to a 17-electron configuration would require an energetically costly (for Cr^{III}) electron-pairing process.^{56–58} A likely alternative is acetate group transfer from the β -C atom of the radical chain to the Cr center, as shown in Scheme 4. Unfortunately, we were unable to observe vinyl chain end resonances in the ¹³C NMR spectrum of the polymer isolated from thermolysis of **8** in vinyl acetate to provide additional support for the mechanism proposed in Scheme 4. Homolytic bond rupture followed by atom (or group) transfer has been observed for R-Co-(porphyrin) complexes where the coordination geometry has no *cis* vacant site available to accommodate the migrating atom or group.⁵⁹ It is quite possible that, following a 2,1-insertion, the resulting CH₂-terminated radical undergoes competitive β -acetate transfer, as shown in Scheme 4, or Cr^{III}–C bond formation, as shown in Scheme 3, thus yielding a mixture of acetate complex and a less active Cp(nacnac^{xyl,xyl})Cr-CH₂CH(OAc)-PVAc dormant species. Only upon warming can the latter be reactivated and eventually be completely transformed into the final acetate product.

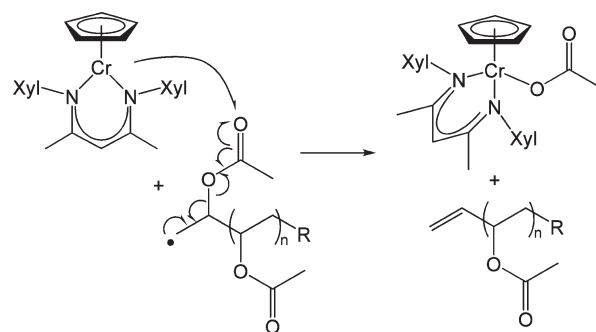
(56) Poli, R. *Chem. Rev.* **1996**, *96*, 2135–2204.

(57) Fettinger, J. C.; Mattamana, S. P.; Poli, R.; Rogers, R. D. *Organometallics* **1996**, *15*, 4211–4222.

(58) Mattamana, S. P.; Poli, R. *Organometallics* **1997**, *16*, 2427–2433.

(59) de Bruin, B.; Dzik, W. I.; Li, S.; Wayland, B. B. *Chem.—Eur. J.* **2009**, *15*, 4312–4320.

Scheme 4



Conclusions

The present study has revealed a more complex situation than previously appreciated for the OMRP of vinyl acetate mediated by half-sandwich Cr^{II} complexes of type CpCr(nacnac). The new data reported here confirm the steric labilization of the Cr^{III}–PVAc bond, with the more encumbering nacnac^{dipp,dipp} ligand resulting in a faster apparent rate constant for polymer growth than the nacnac^{xyl,xyl} ligand. However, the relatively stronger bond of Cp(nacnac^{xyl,xyl})Cr–PVAc is still sufficiently labile to sustain the OMRP of vinyl acetate even at room temperature. On the other hand, an irreversible deactivation process comes into play, slowly at room temperature and faster upon warming, to yield a new material now firmly identified as the acetate complex CpCr(nacnac^{xyl,xyl})OAc.

Acknowledgment. R.P. thanks the Agence Nationale de la Recherche (contract ANR No. NT05-2_42140) and the Institut Universitaire de France for financial support and the Centre Interuniversitaire de Calcul de Toulouse (CICT, project CALMIP) for granting free CPU time. K.M.S. thanks the Natural Sciences and Engineering Research Council of Canada (NSERC) for financial support and thanks Jeffrey A. Therrien and Julia L. Conway for obtaining single crystals of **3** and **7**, respectively, suitable for X-ray diffraction.

Supporting Information Available: A listing of the Cartesian coordinates and final energies of all calculated complexes, UV–visible spectra of complexes **1**, **2**, **3**, **6**, **7**, **8**, and **9**, and complete crystallographic data for complexes **2**, **3**, **6**, **7**, **8**, and **9**. This material is available free of charge via the Internet at <http://pubs.acs.org>.